ce/papers Proceedings in civil engineering

Ernst & Sohn A Wiley Brand

Full paper

Behaviour of 3D Printed Al7075 Square Hollow Sections in Compression

Eman Mansour[1,2] | Xionfeng Ruan[3] | Barbara Rossi[3] | John Robinson[1] | Arun Arjunan[1] | Marina Bock[4]

Correspondence

Eman Mansour
School of Architecture and Built Environment, University of Wolverhampton, Springfield Campus, WV10 0JP, United Kingdom
Email: e.mansour@wlv.ac.uk.

[1] University of Wolverhampton, Wolverhampton, UK
[2] High Institute for Engineering Technologies / ALmajori, Benghazi, Libya
[3] University of Oxford, Oxford, UK
[4] Aston University, Birmingham, UK

Abstract

High strength Aluminium alloys feature low densities, high strength-to-stiffness ratio, large ductility range and high fracture toughness, all attractive features for applications in industries such as automotive, aerospace and construction. To date, little attention has been given to the performance of 3D-printed high strength Aluminium alloys such as Al7075 due to the inherent challenges in the additive manufacturing process. In this context, the present study reports material (tensile) and stub column (compression) tests on additively manufactured (AM) Al7075 square hollow sections (SHS). Both material and SHS samples were manufactured by Direct Metal Laser Sintering (DMLS), a laser powder-bed fusion (L-PBF) sub-technology that uses metal powder as feedstock and a laser to fuse the feedstock layer by layer. Three newly develop set of process parameters that had successfully led to crack free medium sized samples were employed in this study. The effect of post processing treatments on the mechanical properties of printed Al7075 samples is investigated through the application of two heat treatments and a Hot Isostatics Pressing (HIP) treatment. A total of 33 material samples were manufactured and tested in tension, 6 of which in their as built condition and 27 subject to the above post processing treatments. The tensile test results showed that the Al7075 samples manufactured using the new set of parameters used is unable to produce specimens which can then develop their full tensile resistance. Nine square hollow tubes were subsequently manufactured utilising a selected heat treatment and tested in compression. All tubes successfully develop good compression performance and primarily exhibit failure due to local buckling, which led to the formation of a yield-line-like pattern of cracks, ultimately resulting in the specimens' failure.

Keywords

3D-printing, Al7075, Square Hollow Sections, Stub columns.

1 Introduction

Additive Manufacturing (AM), or 3D printing, is a layer-by-layer fabrication process based on a computer-aided 3D model, as defined by ASTM [1]. With growing industrial interest, AM has expanded to materials like concrete and metals and is applied in many disciplines, including civil, mechanical, automotive, medical, and aerospace fields [2].

The advantages of using AM are numerous, such as greater freedom in design, with the potential to create more complex and larger geometries based on computer-aided design [3], reaching greater material utilization ratio, including the possibility to reduce energy consumed and waste during production [4]. There are currently four main AM technologies for metals utilising different feedstocks: direct energy deposition (DED), powder bed fusion (PBF), binder jetting (BJT) and sheet lamination (SHL).

Laser Powder Bed Fusion (L-PBF) is the most mature and advanced metal Additive Manufacturing (AM) technology and is now commonly utilised in the medical and aero-

https://doi.org/10.1002/cepa.70243 wileyonlinelibrary.com/journal/cepa

space industries [5]. With AM nowadays gaining popularity in construction, it is important to understand if this technology is suitable for construction applications where load bearing demands are needed.

One of the limitations of L-PBF are the powders currently available as they have been mostly developed for biomedical, automotive and aerospace applications. Current metals that can be AM using L-PBF are aluminium, stainless steel, titanium and maraging (tooling) steels. Among these available metal powders, aluminium is of interest for construction applications due it is high strength-to-weight ratio and corrosion resistant properties. The most widely used aluminium alloy that can be reliably additively manufactured using L-PBF is the AlSixMg family [6]. Recent research on the structural performance of AlSi10Mg in circular hollow sections [7] and angles [8] manufactured using Direct Metal Laser Sintering (DMLS), a L-PBG sub-technology, has shown that the AlSi10Mg alloy has excellent material properties and compression behaviour, and proved that the design code for structural aluminium, the EN 1999-1-1 [9] appears to be safe for application to AlSi10Mg.

High-strength aluminium has remained unexplored for construction applications. Scalmalloy® and the 7000 aluminium series such as the Al7075 are two high strength aluminium powders available in the market with several more underway [10]. A major challenge in the additive manufacturing of high-strength aluminum alloys is their tendency to develop porosity and cracks during processing [11]. To address this, process optimization, such as adjusting laser parameters (laser power, scan speed, layer thickness, and hatch spacing), can significantly reduce porosity and enhance printability. Building on in-house developed and optimised process parameters for Al7075 that have led to crack free medium size samples [12], this paper presents Al7075 material and compression tests on square hollow sections (SHS) manufactured using Direct Metal Laser Sintering (DMLS), a L-PBF sub-technology. The influence of various post-processing methods including two heat treatments and one hot isostatic pressing (HIP-ping) process on the structural performance is also examined. The ultimate objective of this study is to assess if the in-house developed process parameters are suitable for structural applications.

2 Production of AM samples

Material coupons and SHS stub columns made of Al7075 were manufactured by DMLS using an EOS M290 metal AM machine at Telford Innovation Campus of the University of Wolverhampton which has a printing volume space of 250 x 250 x 200 mm. The chemical composition of casted Al7075 is given in Table 1 [13] and it is worth pointing out that the Al7075 is recognised as a cast alloy in EN 1999-1-1. In its cast form, the Al7075 has the following nominal mechanical properties: nominal Young's modulus value of E= 71.7 GPa, yield stress of 503 MPa, and ultimate stress of 572 MPa [13,14].

In Robinson et al.[12] paper, twelve sets of process parameters involving laser power, hatch distance and scan speed were investigated. These parameters were developed using design of experiments (DOE) approach. Computer Tomography on samples produced in this study revealed that three sets namely #1, #11 and #12 (hereinafter renamed #1, #2 and #3 as given in Table 2) enabled the successful fabrication of crack free medium-sized components. Further information about the development and optimisation of such process parameters can be found in Robinson et al., [12].

Table 1 Chemical composition of casted Al7075 (wt. %)

Al	Si	Fe	Cu	Mn	Mg	Zn	Ti	Cr
Bal	0.3	0.5	1.6	0.2	2.5	5.26	0.2	0.26

Table 2 Processing parameters used for the additive manufacturing of Al7075 samples in this paper

Set#	Hatch distance (mm)	Laser power (W)	Scan speed (mm/s)
1	0.12	252	690
2	0.14	350	715
3	0.12	253	680

Thirty-three dog-bone coupons and nine SHS stub columns were manufactured using the set of process parameters #1, #2 and #3. All samples were manufactured on aluminium building plates and did not require any supporting structures. The nominal dimensions of the material coupons and SHS tubes are shown in Figure 1. In Figure 1 H and B are the cross-sectional height and width of the tube, t is the thickness, and L is the tube length. All tubes had a B x H dimension of 50 x 50 mm and L of 150 mm. L was selected to be three times the cross-sectional dimension to prevent the effects of overall buckling [7] while allowing local buckling to develop fully. Three thickness t were considered: 1.5 mm, 3 mm and 6 mm. All material coupons were built horizontally with their axes parallel to the build direction (0^0) while all the tubes were built upright (90^0) as shown in Figure 1. Repeated samples were available for material testing while one sample per set of process parameters and thickness was available for stub column testing. Three post processing treatments in form of two heat treatments and a HIP process were applied to the samples prior to testing as explained below. Six material coupons did not undergo any post-process treatment and remained in their "as built" form to be able to examine the effect of post-processing in the material response.

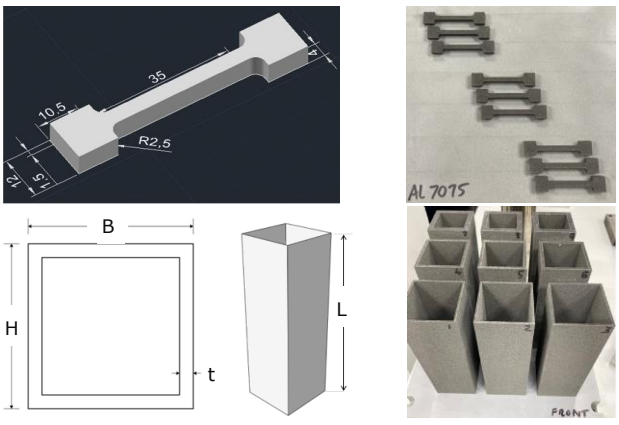

Figure 1 Size designation (left) and material and SHS samples as manufactured on the building plate right.

Heat treatment is one of the key post-processes to improve the mechanical properties of aluminium alloys after AM using L-PBF and including DMLS. Despite this and the current challenges associated with the processing of Al7075, limited studies reporting the effect of heat treatment on the material structure are available [15-18]. Two heat treatments were selected from the literature and applied to the material samples: (i) 160°C for 6h and (ii) 120°C for 72 h. Each treatment was applied to 9 material samples while still attached to the building plate (i.e. three for each set of parameters). Building on the results presented in Section 3, only heat treatment (ii) was applied to the 9 stub columns. Note that thermogravimetric analysis of Al7075 powder has shown that the melting point of Al7075 powder is 650^{0}C, which is significantly higher than the heat treatment temperature. Once material dog-bones and stub columns cooled down at room temperature, they were all were detached from their building plates using electric discharge machining (EDM).

Hot isostatic pressing (HIP) is a material processing method that applies high temperature and pressure to enhances the densification of ceramic and powder metallurgical produced metallic materials and components that ultimately improves material mechanical properties. HIP post-treatment was carried out on 9 dog-bone samples through a commercial service at The Centre of The Quintus Press Design in Sweden, where the samples were subjected to a pressure of 150 MPa at 120°C for 3 hours, then allowed to cool down at room temperature. Prior to HIPping, all samples had already been detached from the building plate using EDM.

3 Experimental programme

A series of tests were performed to determine the tensile behaviour of AM Al7075 using new set of process parameters. Uniaxial tensile testing and CT scanning were performed at Telford Innovation campus of the University of Wolverhampton, while the stub column tests were undertaken at the Sustainable Metal Structures Laboratory of the University of Oxford.

3.1 Nano-computed tomography (CT)

To investigate the influence of AM process parameters and heat treatment on the internal material structure, in particular the presence of cracks and porosity, 4 specimens, one in "as-built" form and three post processed, were scanned using nano-computed tomography (CT) using a Bruker SkyScan 2211 system. Figure 2 shows a cross-section in the middle section in four dog-bone material sample manufactured using set of parameters #3 in "as built" state (a) as well as after applying heat treatment (i) (b), heat treatment (ii) (c) and HIP process (d). The CT scan images show that two types of porosities, metallurgical pores and keyhole pores, are present. The metallurgical pores are typically spherical and small, less than 100 μm in diameter, while keyhole pores are irregular in shape and larger than 100 μm [19]. Keyhole pores and microcracks are present in the "as built" sample as well as in heat treated samples. However, keyholes and pores appear to be smaller in the sample subject to heat treatment (ii) of 120°C for 72h. The CT images also show that HIP significantly densifies the material and minimises micro-cracks and pores substantially, however, these defects are still present. Spherical droplets rather were observed on all sample surfaces, a phenomenon known as 'balling,' common in laser-based processes like DMLS and caused by melt pool instability, which might interfere with geometry measurements.

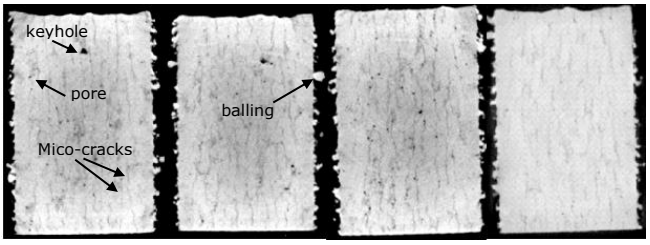

Figure 2 CT scan results of material samples (a) as-built condition (b) after heat treatment at 160^{0}C for 6h (c) 120^{0}C for 72h (d) HIP

3.2 Tensile testing

Tensile tests were carried out in all 33 studied samples to determine the material mechanical properties using a 100kN Zwick Roell servo hydraulic frame equipped with a load cell that measures applied load. An accurately calibrated micro extensometer was used to record deformation during testing, see Figure 4. Measured material properties including Young's modulus (E), ultimate stress (σ_u) and strain at fracture ε_f, are reported in Table 3 for the 6 "as built" samples, 9 samples subject to heat treatment (i), 9 samples subject to heat treatment (ii), and 9 samples subject to HIPping. Two repeated tests were carried out for the "as built batch" while three repeated tests were carried out for the remaining three batches that underwent post processing.

Table 3 Material properties for all coupons – t=6mm

Coupon type	Process #	E (GPa)	σ_u (MPa)	ε_f (%)
As built	#1	11.7	16.20	0.136
		13.4	27.16	0.187
	#2	11.5	9.95	0.089
		10.1	11.73	0.119
	#3	12.7	15.93	0.140
		15.7	23.17	0.147
160°C for 6h	#1	16.7	38.42	0.298
		15.1	43.68	0.545
		15.4	38.31	0.334
	#2	12.5	32.26	0.370
		11.5	31.47	0.389
		12.7	36.24	0.615
	#3	13.8	43.13	0.391
		16.6	42.58	0.430
		17.3	40.47	0.342
120°C for 72h	#1	21.9	34.86	0.225
		20.8	43.12	0.470
		20.4	43.68	0.489
	#2	21.7	38.42	0.559
		20.7	35.34	0.473
		21.8	35.23	0.233
	#3	23.0	37.16	0.447
		22.5	42.81	0.402
		23.2	42.74	0.375
HIP	#1	16.4	43.40	0.531
		16.3	49.12	0.596
		16.5	47.23	0.192
	#2	13.3	41.17	0.681
		17.2	40.97	0.771
		16.7	40.19	0.569
	#3	13.9	49.37	1.526
		18.9	45.61	1.608
		17.4	50.91	0.897

The measured tensile stress-strain curves of the "as built" and post-processed samples are presented in Figure 3. All as-built coupons exhibited brittle behaviour under tensile loading. The stress–strain curves displayed little to no distinct elastic region, transitioning almost immediately into nonlinear behaviour. In contrast, heat-treated coupons showed higher ultimate tensile strength and a greater ductility range on average, consistent with findings reported in [19]. However, all samples, regardless of treatment, demonstrated similarly low tensile strength and limited tensile strain at fracture, with the maximum tensile stress recorded at approximately 45 MPa. This brittle behaviour is primarily attributed to inadequate fusion and a high density of micro-cracks, which compromise the material's integrity under tensile stress. The presence of pores and cracks in the as-built material resulted in lower ultimate strength compared to heat-treated samples [20]. Interestingly, traditional heat treatments, despite not significantly reducing keyhole defects or micro-crack density, led to a notable improvement in ductility.

The results indicate that the AM process, using the current set of parameters, is insufficient to achieve fully melted and properly solidified Al7075 material capable of developing adequate tensile strength. This limitation is consistent with findings reported in the literature [20, 21]. However, until now, tensile testing data for such conditions had not been available. Despite implementing newly developed process parameters that have been shown to improve build quality reducing both porosity and visible surface cracks in medium-scale Al7075 components, the tensile test results presented in this study reinforce earlier concerns. These findings underscore the need for continued process development to enable the reliable additive manufacturing of high-strength Al7075.

3.2 Compression testing

To investigate the compression behaviour of additively manufactured Al7075 SHS, stub column tests were conducted using a 600kN Instron 8804 servo-hydraulic testing frame. Note again that only heat treatment (ii) was applied to the 9 stub columns. Prior to testing, the geometry of all specimens was measured using a digital calliper. Each specimen was coated with matte white spray paint, and two dots spaced 60 mm apart were applied to enable longitudinal strain measurement via a video extensometer. All tests were conducted at a constant displacement rate of 0.5 mm/min. Uniform axial compression was applied using platens, ensuring concentric loading at both end of each specimen as shown in Figure 4.

The measured dimensions of the specimens and the key compression test results, including the ultimate load $F_{u,EXP}$, the end shortening at the ultimate load $\delta_{u,EXP}$, compressive yield stress $\sigma_{0.2}$ and material Young's modulus in compression E_c are reported in Table 4 and 5, respectively.

Table 4 Measured dimensions of stub column tests

Specimen	H (mm)	B (mm)	t (mm)	L (mm)
S50x1.5#1	50.3	50.4	1.51	149.9
S50x1.5#2	50.3	50.3	1.49	148.7
S50x1.5#3	50.3	50.3	1.47	150.1
S50x3#1	50.4	50.4	2.95	149.2
S50x3#2	50.4	50.4	2.88	149.9
S50x3#3	50.5	50.4	3.01	148.5
S50x6#1	50.5	50.5	6.06	148.7
S50x6#2	50.8	50.5	5.98	149.6
S50x6#3	50.3	50.5	5.94	149.6

Table 5 Key results of stub column tests

Specimen	$F_{u,EXP}$ (kN)	$\delta_{u,EXP}$ (mm)	$\sigma_{0.2}$ (N/mm^2)	E_c (GPa)
S50x1.5#1	36.5	1.58	97.8	32.85
S50x1.5#2	37.0	1.84	92.3	33.99
S50x1.5#3	37.0	1.80	94.8	33.44
S50x3#1	151.5	2.74	197.5	32.28
S50x3#2	148.1	2.50	201.8	34.02
S50x3#3	154.0	2.86	229.8	32.78
S50x6#1	378.5	8.08	213.6	26.83
S50x6#2	361.7	7.94	224.4	27.63
S50x6#3	380.0	8.21	232.2	27.70

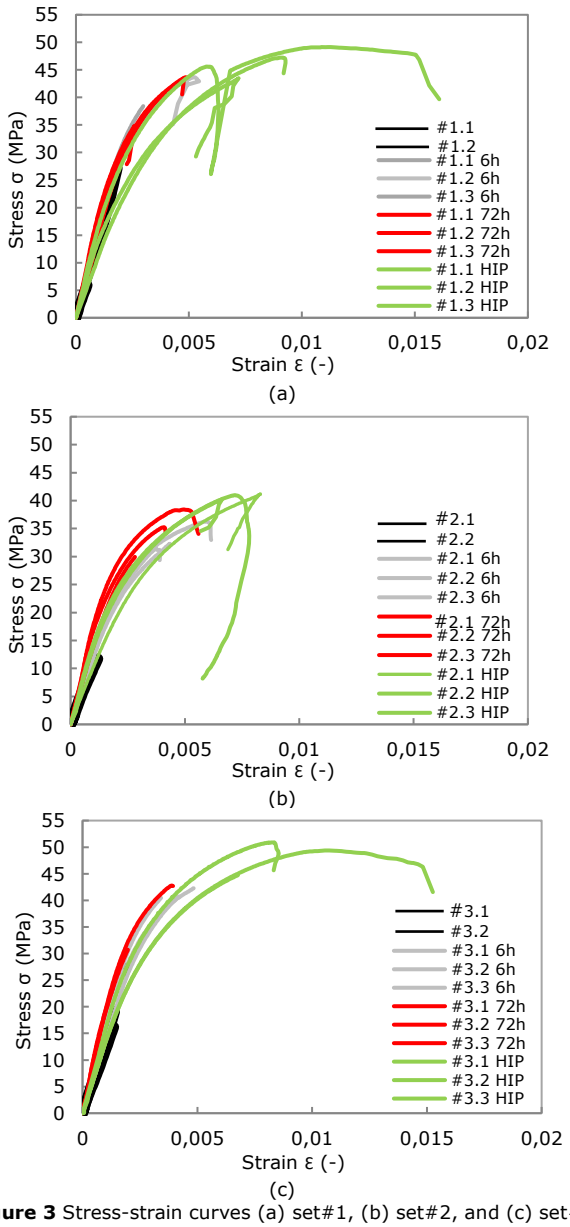

Figure 3 Stress-strain curves (a) set#1, (b) set#2, and (c) set#3

Figure 4 Tensile (left) and compression test set up (right)

All specimens failed due to local buckling with those samples with thickness 1.5 mm and 3 mm exhibiting half-wave local buckling across the faces of the SHS tube. All specimens initially exhibited linear load–displacement behaviour, followed by buckling in a three-halfwave mode, which marked the departure from linearity. The onset of buckling introduced localized tensile stresses. Given the poor tensile resistance of the material, this led to the formation of a yield-line-like pattern of cracks, ultimately resulting in the specimens' failure. In thicker samples, i.e. 6 mm thick, larger plastic strains and material yielding developed followed by cracking after the attainment of the onset of buckling. Figure 5 shows typical failure modes observed while Figure 6 and 7 present the load-displacement and stress-strain curves, respectively. The reported end shortening $\delta_{u,EXP}$ measurement was corrected to remove the deformation of the platens. Overall, the compression behaviour of all tubes was significantly superior to the material tensile behaviour, indicating that, given the current state of AM technology and process understanding, Al7075 is more suitable for structural applications primarily subjected to compressive loads. The different sets of process parameters #1, #2 and #3 did not have a significant impact on the ultimate load although set #3 led to slightly higher compressive loads.

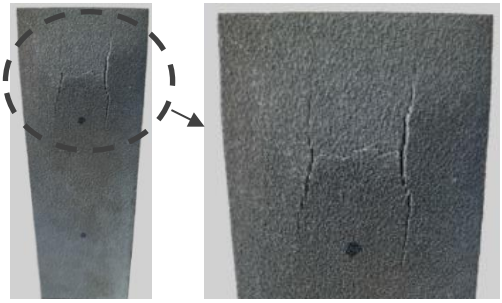

Figure 5 Example of observed Failure modes (left) and cracks developed (right) in S50x3#1

4 Conclusion

This article reported experimental results on additively manufactured Al7075 dog-bone coupons and square hollow section (SHS) stub columns, produced via Direct Metal Laser Sintering with three sets of hatch distances, laser powers, and scan speeds. Samples are subjected to three different post processes. CT scans and tensile tests compared the tensile properties of as built and heat-treated specimens. Results show that the second traditional heat treatment and HIP treatment effectively reduce metallurgical and keyhole porosity, with HIP also decreasing micro-crack density. All heat treatments improved stiffness, ultimate tensile strength, and fracture strain, although further investigations, including SEM analysis, are necessary to confirm these findings.

Stub column tests examined the compressive behaviour of AM Al7075 SHS columns fabricated with the three parameter sets. Failure modes and compressive responses, illustrated in Figures 5-7, resemble those of ductile metal hollow sections, with an initial linear response followed by three-halfwave buckling and yield-line-like fracture patterns leading to failure.

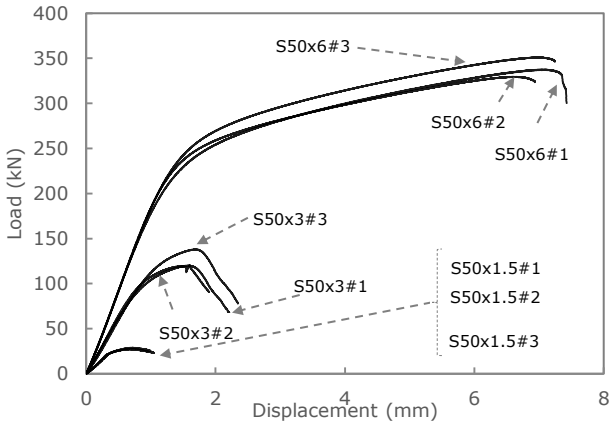

Figure 6 Load-displacement response of SHS

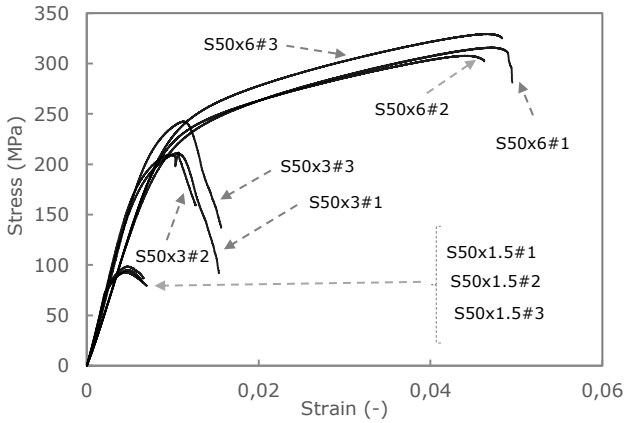

Figure 7 Stress-strain response of SHS

DMLS 3D-printed Al7075 shows strong potential for lightweight construction, but current AM technology faces challenges with porosity and cracking. These issues arise from process limitations, not the alloy itself. Improvement in AM techniques and process optimisation is needed to enable crack-free fabrication of Al7075 components.

Work is currently underway to (a) model the failure modes and failure loads using the Yield Line Theory as an upper-bound analytical approach and (b) model the stub column tests via the finite element method and validate it against the experimental data. This will be followed by a parametric study to generate additional data across a wider range of cross-sectional and member slenderness. Comparison against EN 1999-1-1 design provisions will also be performed.

5 Acknowledgements

This research was funded by the Royal Society Research grants under agreement RSG/R2/222144 awarded to the last author. The first author is grateful to the Ministry of Higher Education of the Libyan Government for their financial contribution. The authors also thank Mr. Neil Bassini, Mr. Andrew Gould and Mr Paul Bates for their assistance in the laboratories of the University of Wolverhampton.

References

[1] *ASTM. Standard terminology for additive manufacturing technologies*. ASTM International, 2012.

[2] Jandyal, A., Chaturvedi, I., Wazir, I., Raina, A., & Haq, M. I. U. (2022). *3D printing–a review of processes, materials and applications in industry 4.0.* Sustainable Operations and Computers, 3, 33-42.

[2] Ninpetch, P.; Kowitwarangkul, P.; Mahathanabodee, S.; Chalermkarnnon, P.; Ratanadecho, P. (2020, October). *A review of computer simulations of metal 3D printing.* In AIP Conference Proceedings (Vol. 2279, No. 1, p. 050002).

[4] Khosravani, M. R., & Reinicke, T. (2020). *On the environmental impacts of 3D printing technology*. Applied Materials Today, 20, 100689.

[5] Singh, R., Gupta, A., Tripathi, O., Srivastava, S., Singh, B., Awasthi, A., ... & Saxena, K. K. (2020). Powder bed fusion process in additive manufacturing: An overview. *Materials Today: Proceedings*, *26*, 3058-3070.

[6] Lasagni, F., Galleguillos, C., Herrera, M., Santaolaya, J., Hervás, D., González, S., & Periñán, A. (2022). *On the processability and mechanical behavior of Al–Mg–Sc alloy for PBF-LB*. Progress in Additive Manufacturing, 7(1), 29-39.

[7] Bock, M., Bawazeer, J., Robinson, J., Theofanous, M., & Skalomenos, K. (2023). *Structural performance of additive manufactured aluminum tubular stub columns.* ce/papers, 6(3-4), 751-756.

[8] Qiu-Yun LI, Jing XU and Ben YOUNG (2024). *Experimental investigation of additively manufactured aluminium alloy angle stub columns*. 10h International Conference on Steel and Aluminium Structures (ICSAS24)

[9] European committee for standardization (EC9), "*Eurocode 9: design of aluminum structures— part 1-1: general rules—general rules and rules for buildings*." BS EN 1999-1-1:2007, CEN., 2007.

[10] Awd, M., Tenkamp, J., Hirtler, M., Siddique, S., Bambach, M., & Walther, F. (2017). *Comparison of microstructure and mechanical properties of Scalmalloy® produced by selective laser melting and laser metal deposition*. Materials, 11(1), 17.

[11] Abdollahi, A., Nganbe, M., & Kabir, A. S. (2022). *On the elimination of solidification cracks in fusion welding of Al7075 by TiC-nanoparticle enhanced filler metal.* Journal of Manufacturing Processes, 81, 828-836.

[12] Robinson, J.; Wanniarachchi, C.; Arjunan, A.; Baroutaji, A.; Singh, M.; Vance, A.; Appiah, M.; Arafat, A. (2025). *The influence of laser powder bed fusion atmospheric oxygen on the thermal conductivity of al7075 aluminium allo*y. Manuscript submitted for publication.

[13] Rajesh, S., Kumar, R. S., Madhankumar, S., Sheshan, M., Vignesh, M., & Kumar, R. S. (2021). *Study of the mechanical properties of Al7075 alloy, silicon of the mechanical properties of Al7075 alloy, silicon carbide and fly ash composites manufactured by stir casting technique*. Materials Today: Proceedings, 45, 6438-6443

[14] Koria, C. S., Kumar, R., & Chauhan, P. S. (2023, May). *Reinforcement of micro and nano material with aluminum alloy (Al7075) metal matrix composite: A review*. In Journal of Physics: Conference Series (Vol. 2484, No. 1, p. 012023). IOP Publishing.

[15] Stopyra, W., Gruber, K., Smolina, I., Kurzynowski, T., & Kuźnicka, B. (2020*). Laser powder bed fusion of AA7075 alloy: Influence of process parameters on porosity and hot cracking*. Additive Manufacturing, 35, 101270.

[16] Li, G., Jadhav, S. D., Martín, A., Montero-Sistiaga, M. L., Soete, J., Sebastian, M. S., ... & Vanmeensel, K. (2021*). Investigation of solidification and precipitation behavior of Si-modified 7075 aluminum alloy fabricated by laser-based powder bed fusion.* Metallurgical and Materials Transactions A, 52, 194-210.

[17] Li, M., Yao, S., Wang, J., Chen, Z., Zhang, G.,Zhang, S., & Li, Y. (2022). *Role of Er on the densification, microstructure and mechanical properties of 7075 aluminium alloys manufactured by laser powder bed fusion*. Journal of Materials Research and Technology, 20, 2021-2033.

[18] Zhang, K., Wenner, S., Marioara, C. D., Hovig, E. W., Du, Q., Onsøien, M., & Marthinsen, K. (2024, August). *Additive manufacturing of 7xxx aluminium alloys by laser powder bed fusion*. In IOP Conference Series: Materials Science and Engineering (Vol. 1310, No. 1, p. 012019). IOP Publishing.

[19] Aboulkhair, N. T. (2016). *Additive manufacture of an aluminium alloy: processing, microstructure, and mechanical properties* (Doctoral dissertation, University of Nottingham).

[20] Ellis, C. R. (2019). *Additive powder manufacture of new aluminium alloys* (Doctoral dissertation, University of Warwick).

[21] Montero-Sistiaga, M. L., Mertens, R., Vrancken, B., Wang, X., Van Hooreweder, B., Kruth, J. P., & Van Humbeeck, J. (2016). *Changing the alloy composition of Al7075 for better processability by selective laser melting.* Journal of Materials Processing Technology, 238, 437-445.